NON-DARCY NATURAL CONVECTION IN A HIGH POROSITY MEDIUM HEATED FROM BELOW: EFFECTS OF THERMAL DISPERSION AND LOCAL THERMAL NON-EQUILIBRIUM - PART 1. NUMERICAL FORMULATION AND VALIDATION

M.S. Phanikumar – phani@msu.edu
Departments of Geological Sciences and Civil & Environmental Engineering
Michigan State University – East Lansing, MI, USA

R.L. Mahajan – mahajan@spot.colorado.edu
CAMPMode (Center for Advanced Manufacturing and Packaging
of Microwave, Optical and Digital Electronics)
Department of Mechanical Engineering
University of Colorado, Boulder, CO, USA

Abstract. *In this two-part paper, we present numerical solutions for buoyancy induced flows in high porosity metal foams heated from below. Experiments conducted under natural convection conditions for the same configuration were used to validate the numerical model. The results show enhancement in heat transfer for different metal foam - fluid combinations. Thermal dispersion effects and the effects of Darcy number on heat transfer are reported. Conditions under which the local thermal equilibrium (LTE) assumption can introduce significant errors are also discussed.*

Keywords: *Metal Foams, Enhancement, Thermal Non-Equilibrium, Dispersion*

1. INTRODUCTION

High porosity metal foams ($\varepsilon > 0.85$) have gained attention in recent years as potentially excellent candidates for meeting the high thermal dissipation demands in the electronic industry. The mechanisms that contribute to the enhanced heat transfer include heat conduction in the metal foam matrix (whose conductivity is usually several orders of magnitude higher compared to the fluid conductivity), and thermal dispersion in the fluid at high velocities. The dispersion conductivity accounts for the effects of pore-level hydrodynamics on the macroscopic transport and essentially represents the enhanced mixing due to the presence of the solid phase.

The well-known Darcy's law is based on a balance between the pressure gradient and the viscous forces and breaks down for high velocities when inertia terms are no longer negligible. Non-Darcian effects become particularly important in metal foams as the fluid moves in tortuous paths and eddies are shed behind the solid fibers in the interstitial pore volume. The resulting pressure drop across the medium and the increased mixing (or dispersion) accounts for an increase in the net transport. Earlier efforts to quantify effects of dispersion were mostly confined to packed beds. Relevant to metal foams is the work of Hunt and Tien (1988) which

showed that, for forced convection, significant augmentation in heat transfer takes place due to thermal dispersion. More recent studies aimed at understanding effects of thermal dispersion in forced convection have also shown an increase in heat transfer with the inclusion of thermal dispersion (Amiri and Vafai, 1994; Amiri et al., 1995; Hsiao, 1998, Calmidi, 1998, Calmidi and Mahajan, 2000). Jiang et al. (1999) found that, if thermal dispersion effects are ignored for forced convection in water, then the numerically predicted heat transfer results are lower compared to the experimental results.

The aim of this paper is to present numerical results for buoyancy-induced flow in a high porosity metal foam sample heated from below and placed in a region surrounded by air. Energy transport in porous media is generally studied by invoking the assumption of local thermal equilibrium (LTE). The validity of this assumption for the case of metal foams is doubtful in view of the vastly different thermal conductivities encountered for the metal foam -- fluid combinations. Consequently, the effects of local thermal non-equilibrium (LTNE) are studied by using a two-equation model for energy. Such an approach was followed earlier, among others, by Amiri and Vafai (1994), Amiri et al., (1995), Jiang et al. (1999) and Nield and Kuznetsov (1999), Calmidi (1998) and Calmidi and Mahajan (2000). Finally, limited experimental data in support of the numerical simulation, is also presented.

2. ANALYSIS

Consider a two-dimensional metallic foam sample heated from below. The metal foam is surrounded by an air region with an imaginary boundary extending a distance s_1 in the x-direction and s_2 in the y-direction. The governing equations for the fluid and porous media are written separately. For the ambient air domain we have:

Continuity and Momentum:

$$\frac{\partial u}{\partial x}+\frac{\partial v}{\partial y}=0 \tag{1}$$

$$u\frac{\partial u}{\partial x}+v\frac{\partial u}{\partial y}=\rho_a^{-1}\left(\frac{\partial p}{\partial x}\right)+\frac{\partial}{\partial x}\left(\mu_a\frac{\partial u}{\partial x}\right)+\frac{\partial}{\partial y}\left(\mu_a\frac{\partial u}{\partial y}\right) \tag{2}$$

$$u\frac{\partial v}{\partial x}+v\frac{\partial v}{\partial y}=\rho_a^{-1}\left(\frac{\partial p}{\partial y}\right)+\frac{\partial}{\partial x}\left(\mu_a\frac{\partial v}{\partial x}\right)+\frac{\partial}{\partial y}\left(\mu_a\frac{\partial v}{\partial y}\right)+\rho g\beta(T-T_\infty) \tag{3}$$

Energy equation for air:

$$\rho_a c_{pa}\left(u\frac{\partial T}{\partial x}+v\frac{\partial T}{\partial y}\right)=\frac{\partial}{\partial x}\left(k_a\frac{\partial T}{\partial x}\right)+\frac{\partial}{\partial y}\left(k_a\frac{\partial T}{\partial y}\right) \tag{4}$$

where u,v are the velocoty components in the x and y directions, T is the temperature and the subscripts a and ∞ denote the conditions for air and ambient respectively. For the porous

medium the governing equations for the non-Darcian model were derived following the well-known volume averaging procedure for porous media (Whitaker, 1967; Vafai and Tien, 1981). The macroscopic momentun equations governing the present problem and the solid and fluid phase energy equations can be written as follows.

Continuity and Momentum:

$$\nabla \cdot \langle \mathbf{v} \rangle = 0 \tag{5}$$

$$\frac{\rho_f}{\varepsilon^2} \langle \mathbf{v} \rangle \cdot \nabla \langle \mathbf{v} \rangle = -\nabla \langle p \rangle^f + \rho_f \mathbf{g} + \frac{\mu}{\varepsilon} \nabla^2 \langle \mathbf{v} \rangle - \frac{\mu}{K} \langle \mathbf{v} \rangle - \frac{C}{K^{1/2}} \rho_f |\langle \mathbf{v} \rangle| \langle \mathbf{v} \rangle - \mathbf{g} \beta (\langle T_f \rangle^f - T_\infty) \tag{6}$$

Energy Equation for the Fluid:

$$\langle \rho_f \rangle^f c_{pf} \langle \mathbf{v} \rangle \cdot \nabla \langle T_f \rangle^f = \nabla \cdot \left\{ (k_{fe} + k_d) \cdot \nabla \langle T_f \rangle^f \right\} + h_{sf} a_{sf} (\langle T_s \rangle^s - \langle T_f \rangle^f) \tag{7}$$

Energy Equation for the Solid Matrix:

$$0 = \nabla \cdot \left\{ k_{se} \cdot \nabla \langle T_s \rangle^s \right\} - h_{sf} a_{sf} (\langle T_s \rangle^s - \langle T_f \rangle^f) \tag{8}$$

In the momentum equation (6), the last three terms are the Brinkman (or friction) term, the Darcy term and the Forchheimer (or inertia) term. The notation $\langle \phi \rangle$ is used to denote the local volume average of a quantity while $\langle \phi \rangle^\gamma$ denotes the intrinsic phase average of the same quantity for phase γ while the subscripts s and f denote solid and fluid respectively. The effective conductivities k_{eff}, k_{se} and k_{fe} are functions of the geometry of the medium and the individual conductivities k_s and k_f respectively. In the above, C denotes the geometric function, h_{sf} is the interfacial heat transfer coefficient between the solid matrix and the fluid, and a_{sf} is the specific surface area of the foam sample defined as the total interstitial surface area of the pores per unit bulk volume (Bear, 1972) and calculated based on geometrical considerations (Calmidi, 1999) as:

$$a_{sf} = \frac{3\pi d_f}{d_p^{\,2}} \tag{10}$$

Here d_p is the pore-size and d_f is the fiber diameter. Pore size refers to the size of the pores which are in the shape of a dodecahedron and is usually expressed in units of pores per inch (PPI). The fibers of the metal foam form the edges of a dodecahedron with about 12-14 sides and the cross section of the fiber is circular only for low porosity values. The porosity ε, pore size d_p and the fiber diameter d_f are related. Since the geometry of metal foams is considerably complex, workable approximations have been derived based on simpler models (Calmidi, 1999). The following equation from Calmidi (1999) is based on one such model and is used in the present work.

$$\frac{d_f}{d_p} = 1.18\sqrt{\frac{1-\varepsilon}{3\pi}}\left(\frac{1}{1-\exp(-(1-\varepsilon)/0.04)}\right) \qquad (11)$$

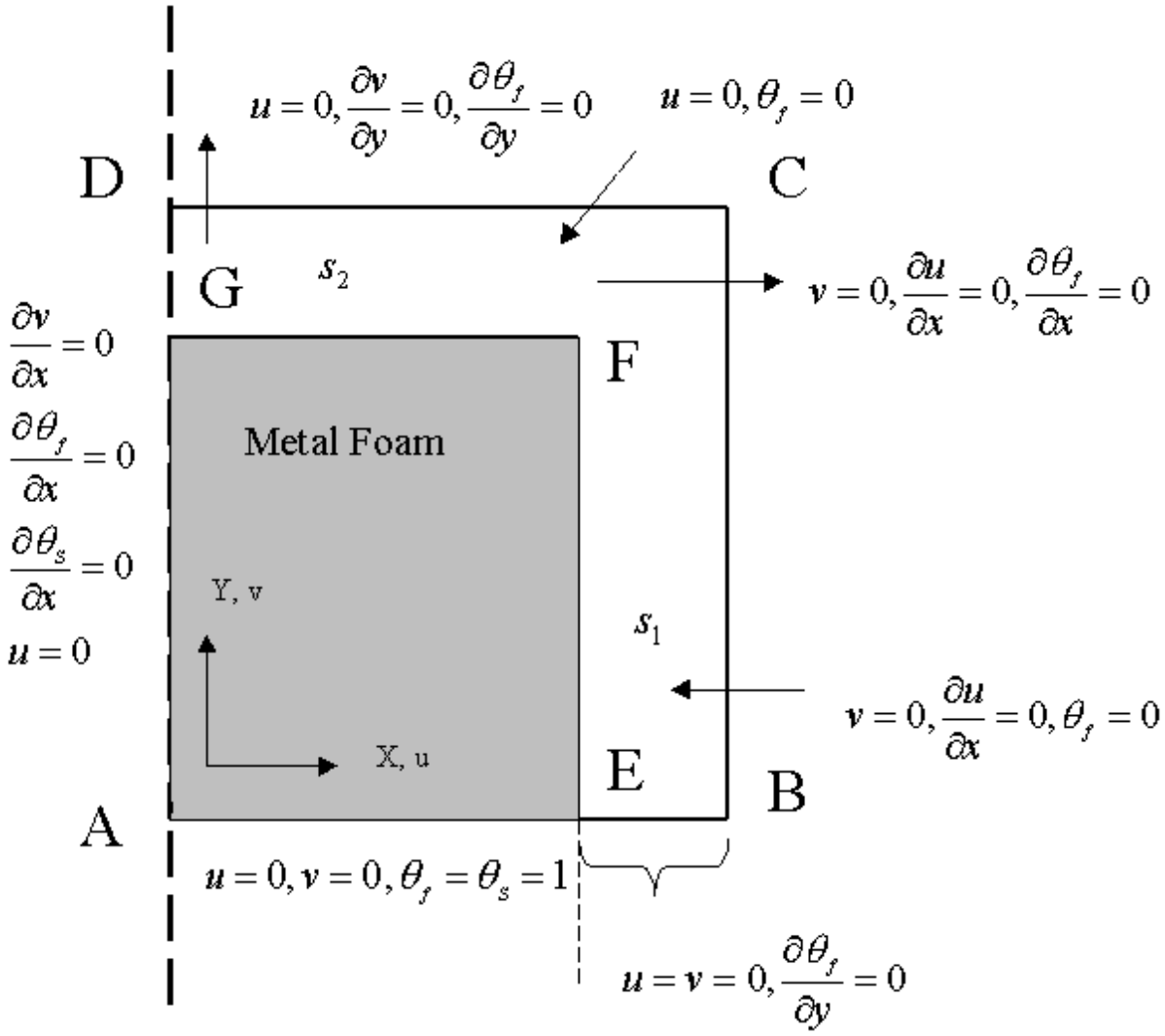

Figure 1 Definition Sketch and Boundary Conditions

The interfacial heat transfer coefficient for packed beds is usually calculated using a correlation due to Wakao et al. (1979) although no such general correlation exists for foamed materials. In view of the fact that the radial temperature gradients are expected to be small for metal foams, it is reasonable to use an appropriate Nusselt number correlation for flow over an external body to calculate h_{sf} . For example, Sathe et al. (1990) used the heat transfer coefficient for a cylinder in cross flow in the study of porous radiant burners. For the present problem the natural convection velocity $\left|\langle \mathbf{v} \rangle\right|$ can be used to calculate a Reynolds number based on the fiber diameter ($=\left|\langle \mathbf{v} \rangle\right| \cdot d_f / \nu \cdot \varepsilon$) and then h_{sf} can be calculated using a forced convection correlation. This is based on the assumption that the natural convection velocity at a point essentially becomes a

forced flow for a fiber at that location. For most of the cases considered in the present work, the range of fiber Reynolds numbers (Re_d) was less than 5000. For this range the following correlation proposed by Zhukauskas (1972) can be used to estimate h_{sf}:

$$\overline{Nu}_d = \frac{h_{sf} \cdot d_p}{k_f} = \begin{cases} 0.75\,\mathrm{Re}_d^{\,0.40}\,\mathrm{Pr}^{0.37}, 1 \le \mathrm{Re}_d \le 40 \\ 0.51\,\mathrm{Re}_d^{\,0.51}\,\mathrm{Pr}^{0.37}, 40 \le \mathrm{Re}_d \le 1000 \end{cases} \qquad (12)$$

The above correlation is strictly valid for circular cylinders. For a metal foam, the cross-section of the fibers is circular only for low porosity values. As the porosity increases (> 0.9), the fiber cross-section changes from being circular to almost triangular Since interest in the present work is confined to high porosity values, we need a correlation that takes this fact into account. However, a closer examination of the heat transfer correlations for external flow over bodies of different cross-sections (Incropera, 1997) showed that an equation of the form

$$\overline{Nu}_d = C_T \cdot \mathrm{Re}_d^{\,m}\,\mathrm{Pr}^{0.37} \qquad (13)$$

can be used for non-circular cross-sections and that the exponent m varies much more slowly compared to the constant C_T. The exponent *m* was found to lie between 0.5 and 0.78 depending on the cross-section and the Reynolds number. Since the fiber Reynolds numbers encountered in the present work are less than 10^3, we have decided to study the effect of the fiber cross-section on the heat transfer by replacing equation (12) with equation (13) and by using different values for C_T while using a constant value of $m = 0.51$ for the exponent. The results of this study are presented later.

The effective thermal conductivity of the porous medium (k_{eff}) as well as the effective conductivities for the solid and the fluid phases(k_{se} and k_{fe}) depend on the porosity ε, geometry of the metal foam and the individual conductivities of the solid and the fluid (k_s and k_f respectively). These quantities were evaluated using the following expressions proposed by Calmidi and Mahajan (1999):

$$k_{eff} = \left(\left(\frac{2}{\sqrt{3}} \right) \left(\frac{r\left(\frac{b}{L}\right)}{k_f + \left(1 + \frac{b}{L}\right)\frac{(k_s - k_f)}{3}} + \frac{(1-r)\left(\frac{b}{L}\right)}{k_f + \frac{2}{3}\left(\frac{b}{L}\right)(k_s - k_f)} + \frac{\frac{\sqrt{3}}{2} - \frac{b}{L}}{k_f + \frac{4r}{3\sqrt{3}}\left(\frac{b}{L}\right)(k_s - k_f)} \right) \right)^{-1}$$

$$\frac{b}{L} = \frac{-r + \sqrt{r^2 + \frac{2}{\sqrt{3}}(1-\varepsilon)\left(2 - r\left(1 + \frac{4}{\sqrt{3}}\right)\right)}}{\frac{2}{3}\left(2 - r\left(1 + \frac{4}{\sqrt{3}}\right)\right)} \qquad (14)$$

In the above equations (b/L) and r are functions of the metal foam geometry while k_s and k_f denote the conductivities of the individual phases (solid and fluid respectively). A value of $r = 0.09$ was found to produce an excellent agreement with the experimentally measured values of conductivity for metal foams. The effective conductivities for the solid and the fluid (k_{se} and k_{fe}) can be obtained as special cases from the above equation by setting $k_f = 0$ and $k_s = 0$ respectively. All computations reported in this paper used the dimensions of the metal foam sample from the experiments - 2.5″ (Length) x 2.0″ (Height).

In our work, the dispersion is treated as an additional contribution to the stagnant diffusive component as shown in equations (3) and (4) (Hunt and Tien (1988), Amiri and Vafai(1994)). In an earlier analysis, Koch and Brady (1986) used ensemble averaging and defined the dispersion as the product of the velocity, fiber thickness and a constant dependent on the porosity. Using this approach, the dispersion coefficient can be written as:

$$k_d = \rho c_p C_D \sqrt{K} \cdot |\mathbf{v}| \qquad (15)$$

Since the metal foam matrix is isotropic, we assume that the *x* and *y* components of dispersion are equal (i.e., $k_{dx} = k_{dy} = k_d$). The coefficient of thermal dispersion C_D requires determination and is described later.

The above model for dispersion does not account for wall effects directly, except through the change in the velocity profile near the wall. For packed beds, Cheng (1986) proposed the use of a wall function to account for the reduced mixing and hence, reduced dispersion close to the wall. The length scaling for this case, is however, based on the Brinkman screening length (~ O($\sqrt{K}$)) which is very small for metal foams. Consequently, a wall function is not used in the present work as the reduced velocity near the wall is expected to account for the reduced dispersion.

The boundary conditions for the above set of equations are shown in Figure 1. In view of the symmetry in the problem, it is sufficient if we solve only one half of the domain. We consider the right half of the domain and consequently, the left edge AD becomes a line of symmetry as shown in Figure 1. No-slip conditions are imposed on the bottom surface (AB). Conditions on the two imaginary boundaries (BC and CD) are specified so as to allow air to cross these boundaries freely (locally parabolic assumption). The two sets of equations for the air and porous regions are coupled at the two interfaces (EF and FG) by the following matching conditions.

For the interface in the x - direction:

$$T\big|_{x=L^-} = T\big|_{x=L^+} \qquad (16a)$$

$$-k_{eff}\left.\frac{\partial T}{\partial x}\right|_{x=L^-} = -k_a\left.\frac{\partial T}{\partial x}\right|_{x=L^+} \tag{16b}$$

$$u|_{x=L^-} = u|_{x=L^+} \tag{16c}$$

$$v|_{x=L^-} = v|_{x=L^+} \tag{16d}$$

$$p|_{x=L^-} = p|_{x=L^+} \tag{16e}$$

$$\mu_{eff}\left.\frac{\partial u}{\partial x}\right|_{x=L^-} = \mu\left.\frac{\partial u}{\partial x}\right|_{x=L^+} \tag{16f}$$

$$\mu_{eff}\left(\frac{\partial v}{\partial x}+\frac{\partial u}{\partial y}\right)_{x=L^-} = \mu\left(\frac{\partial v}{\partial x}+\frac{\partial u}{\partial y}\right)_{x=L^+} \tag{16g}$$

For the interface in the y - direction:

$$T|_{y=H^-} = T|_{y=H^+} \tag{17a}$$

$$-k_{eff}\left.\frac{\partial T}{\partial y}\right|_{y=H^-} = -k_a\left.\frac{\partial T}{\partial y}\right|_{y=H^+} \tag{17b}$$

$$u|_{y=H^-} = u|_{y=H^+} \tag{17c}$$

$$v|_{y=H^-} = v|_{y=H^+} \tag{17d}$$

$$p_{y=H^-} = p|_{y=H^+} \tag{17e}$$

$$\mu_{eff}\left.\frac{\partial v}{\partial y}\right|_{y=H^-} = \mu\left.\frac{\partial v}{\partial y}\right|_{y=H^+} \tag{17f}$$

$$\mu_{eff}\left(\frac{\partial v}{\partial x}+\frac{\partial u}{\partial y}\right)_{y=H^-} = \mu\left(\frac{\partial v}{\partial x}+\frac{\partial u}{\partial y}\right)_{y=H^+} \tag{17g}$$

Conditions (a)- (e) above express the continuity of temperature, heat flux, normal and tangential velocities and the pressure respectively while conditions (f) - (g) match the deviative normal and shear stresses at the interface. Equations (g) represent an extension of the shear stress matching condition due to Neale and Nader (1974) for flow which is not parallel to the interface. Vafai and Thiagaraja (1987) showed that this matching condition can be used at the interface only when the Brinkman shear term is included in the momentum equation. In the above equations μ_{eff} is an effective viscosity of the porous medium and is associated with the Brinkman term in the momentum equation. Determination of μ_{eff} remains an open problem (Givler and Altobelli, 1994). Results obtained by assuming $\mu_{eff} = \mu$ were found to be in good agreement with experimental studies (Beckermann et al, 1987, Sathe et al., 1988). This approach is adopted in the present work. Matching the heat flux at the interfaces becomes a non-trivial task when the solid and fluid phase equations are solved separately. We are not aware of any earlier work in which heat flux was matched at a fluid-porous interface (with a finite velocity) while using the two-equation model for energy. The difficulty was noted earlier by Amiri et al. (1994) while

specifying a heat-flux boundary condition in a porous channel and more recently by Nield and Kuznetsov (1999). Neither of these papers, however, deals with a fluid-porous interface. The issue is related to the fact that it is not obvious how the flux from the porous medium gets divided between the solid and fluid phases so that it can be equated to the flux from the air side. It is possible to think of different scenarios here. In one scenario, if we assume that heat is dominantly transported to the interfaces by conduction in the solid matrix due to the high conductivity of metal foams and subsequently convected away, then local thermal equilibrium (LTE) can be assumed at the interfaces giving a single temperature for the solid, fluid and the air:

$$T_f = T_a = T_S \tag{18a}$$

Each of the individual fluxes for the solid and the fluid phases can be assumed to be in balance with the flux for the air region as shown below for the interface at $x = L$:

$$\begin{aligned} -k_{eff}\left.\frac{\partial T_f}{\partial x}\right|_{x=L^-} &= -k_a\left.\frac{\partial T_a}{\partial x}\right|_{x=L^+} \\ -k_{eff}\left.\frac{\partial T_s}{\partial x}\right|_{x=L^-} &= -k_a\left.\frac{\partial T_a}{\partial x}\right|_{x=L^+} \end{aligned} \tag{18b}$$

The single-domain approach used in the present work satisfies equations (18a) and (18b). The above approach was found to provide an excellent agreement between the model predictions and the experimental data under a wide range of conditions.

3. DIMENSIONLESS EQUATIONS

The governing equations for the fluid and porous regions were solved using a unified one-domain approach. The advantage of such a formulation lies in the fact that it automatically ensures the satisfaction of the interfacial conditions. In addition, it does not involve complicated inner iteration loops for values at the interface (Beckermann et al., 1987; Vafai and Kim, 1994). Consequently, the two sets of equations for the fluid and the porous regions are combined into one set by using the following binary flag:

$$\delta(x,y) = \begin{cases} 1 & \text{for metal foam} (0 \le \varepsilon \le 1) \\ 0 & \text{for air region } (\varepsilon = 1) \end{cases} \tag{19}$$

We drop the $\langle\phi\rangle$ notation for convenience and make the above equations dimensionless by employing the following scales: H for length, $(T_h - T_\infty)$ for temperature, (α_f / H) for velocity, (H^2/α_f) for time and $(H^2/\rho\cdot\alpha^2)$ for pressure. The resulting dimensionless equations using primitive variables appear as shown below.

$$\begin{aligned} \frac{1}{\varepsilon^2}\left(u\frac{\partial u}{\partial x} + v\frac{\partial u}{\partial y}\right) = &-\frac{\partial p}{\partial x} - \frac{Pr}{Da}u\delta - \frac{C}{\sqrt{Da}}|\tilde{\mathbf{v}}|u\delta \\ &+ \varepsilon^{-1}\{\delta\cdot Pr + (1-\delta)\cdot Pr_a\}\nabla^2 u \end{aligned} \tag{20}$$

$$\frac{1}{\varepsilon^2}\left(u\frac{\partial v}{\partial x}+v\frac{\partial v}{\partial y}\right)=-\frac{\partial p}{\partial y}-\frac{Pr}{Da}v\delta-\frac{C}{\sqrt{Da}}|\tilde{\mathbf{v}}|v\delta+\varepsilon^{-1}\{\delta\cdot Pr+(1-\delta)\cdot Pr_a\}\nabla^2 v+\{\delta Ra_f+(1-\delta)Ra_a\}\cdot\theta \tag{21}$$

Energy Equation for the Fluid and Air:

$$\left(u\frac{\partial\theta_f}{\partial x}+v\frac{\partial\theta_f}{\partial y}\right)=\frac{Bi_f\cdot\lambda_f\cdot\delta}{\sqrt{Da}}(\theta_s-\theta_f)+\frac{\partial}{\partial x}\left[\left\{\delta\left(\lambda_f+C_D\sqrt{Da}\cdot\sqrt{u^2+v^2}\right)+(1-\delta)\lambda_a\right\}\frac{\partial\theta_f}{\partial x}\right]+\frac{\partial}{\partial y}\left[\left\{\delta\left(\lambda_f+C_D\sqrt{Da}\cdot\sqrt{u^2+v^2}\right)+(1-\delta)\lambda_a\right\}\frac{\partial\theta_f}{\partial y}\right] \tag{22}$$

Energy Equation for the Solid Matrix:

$$0=\lambda_s\delta\left[\frac{\partial^2\theta_s}{\partial x^2}+\frac{\partial^2\theta_s}{\partial y^2}\right]-Bi_s\cdot\lambda_s\,\delta(\theta_s-\theta_f) \tag{23}$$

The dimensionless quantities appearing in the above equations are defined as shown below.

$$Da=\frac{K}{H^2},Bi_s=\frac{h_{sf}a_{sf}H^2}{k_{se}},Bi_f=\frac{h_{sf}a_{sf}H\sqrt{K}}{k_{fe}},$$

$$\lambda_f=\frac{k_{fe}}{k_f},\lambda_s=\frac{k_{se}}{k_f},\lambda_a=\frac{k_a}{k_f}, \tag{24}$$

$$Ra_f=\frac{g\beta H^3(T_h-T_\infty)}{\upsilon_f\alpha_f},Ra_a=\frac{g\beta H^3(T_h-T_\infty)}{\upsilon_a\alpha_a}$$

The dimensionless boundary conditions are shown in Figure 1. The interface matching conditions are not shown in dimensionless form for the sake of brevity as they can be easily derived from (14)-(15). Heat transfer from the heated wall occurs both through the solid phase and the liquid phase. The total heat transfer can be written as,

$$q=\bar{h}L\Delta T=\int_0^L\left(k_{se}\frac{\partial T_s}{\partial y}+k_{fe}\frac{\partial T_f}{\partial y}\right)dx \tag{25}$$

$$\overline{Nu}=\frac{\bar{h}L}{k_{eff}}=\int_0^A\left(\frac{k_{se}}{k_{eff}}\frac{\partial\theta_s}{\partial y}+\frac{k_{fe}}{k_{eff}}\frac{\partial\theta_f}{\partial y}\right)dx=\overline{Nu}_s+\overline{Nu}_f \tag{26}$$

We note that the above definition of the total Nusselt number is not suitable if one is interested in the heat transfer augmentation that results from using the metal foam (compared to the case in which there is no metal foam). For that case, it is more convenient to define a second Nusselt

number that is based on the fluid conductivity rather than the effective conductivity of the porous medium. This quantity is defined as:

$$\overline{Nu_f} = \frac{\overline{h_f} L}{k_f} = \int_0^A \left(\frac{k_{se}}{k_f} \frac{\partial \theta_s}{\partial y} + \frac{k_{fe}}{k_f} \frac{\partial \theta_f}{\partial y} \right) dx = \int_0^A \left(\lambda_s \frac{\partial \theta_s}{\partial y} + \lambda_f \frac{\partial \theta_f}{\partial y} \right) dx \quad (27)$$

Similarly, the Nusselt number corresponding to the case in which there is no metal foam can be defined as:

$$\overline{Nu_0} = \frac{\overline{h}_0 L}{k_f} = \int_0^A \frac{\partial \theta_f}{\partial y} dx \quad (28)$$

The percentage enhancement in heat transfer resulting from the use of the metallic foam can then be defined as:

$$\%E = \frac{\left(\overline{Nu_f} - \overline{Nu_0}\right)}{\overline{Nu_0}} \times 100 \quad (29)$$

Unless mentioned otherwise, all subsequent references are to the total Nusselt number as defined in equation (26).

4. NUMERICAL METHOD

The above system of equations and boundary conditions have been solved using control volume based, semi-implicit methods (Patankar, 1980). The control volume formulation ensures conservation of momentum and energy as well as continuity of fluxes. The harmonic mean formulation of Patankar was used to describe the diffusion coefficients at the porous-fluid interfaces. This formulation can handle abrupt changes in the properties (such as permeability) across the interface without requiring an excessively fine grid. A staggered, non-uniform grid and the power-law scheme were used. The velocity – pressure coupling was handled using the SIMPLER algorithm. The non-uniform grid enabled the placement of fine steps at the porous-fluid interface and at the boundaries. All computations reported in this paper were carried out using a 101 x 101 non-uniform grid after carrying out a careful grid dependence study. For this level of grid refinement, the uncertainty in the average Nusselt number reported is not greater than 3%. The width of the air domain was increased till the difference in the Nusselt number is less than 1%. A value of 1.0 was finally used for the dimensionless width of the air domain in both the x and y directions. The stopping criterion for the computations was based on the requirement that the relative error in all variables between two successive iterations must be less than 1.0×10^{-5}.

4. RESULTS AND DISCUSSION

To validate the present model, including the treatment of the interface, we have compared our model results with the work of Beckermann et al. (1987) for natural convection in a rectangular

enclosure in which there is a fluid-porous interface. A very good overall agreement is obtained and the average Nusselt numbers are in excellent agreement. Figure 2 shows a comparison of the dimensionless temperature profiles for one case.

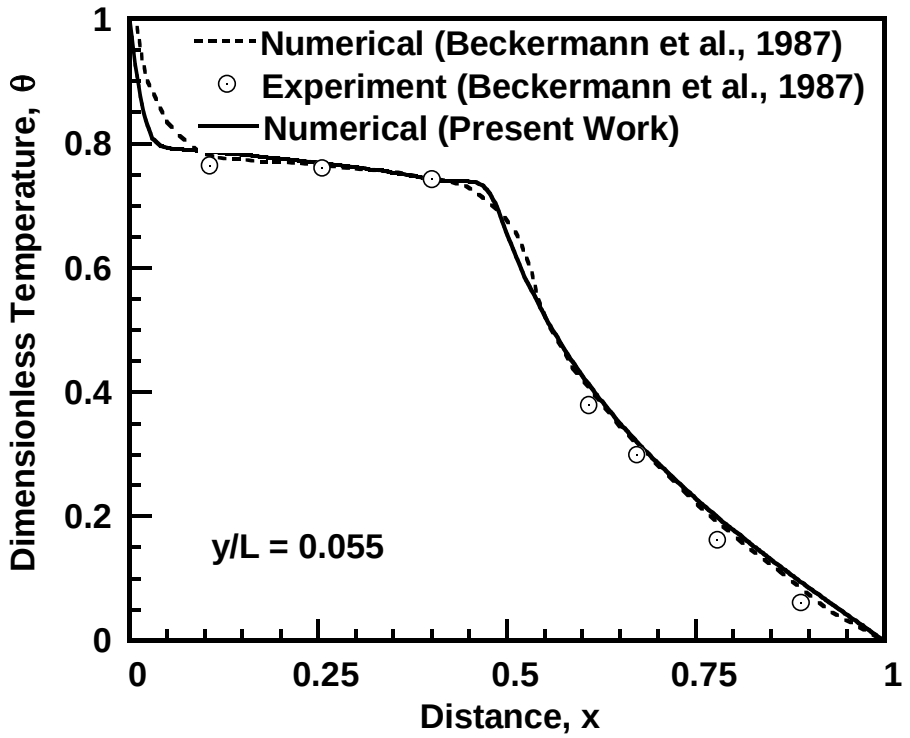

Figure 2. Comparison of present numerical results (dimensionless temperature) with the work of Beckermann et al. (1987) for flow in an enclosure in the presence of an interface. The interface is located at x = 0.5.

5. CONCLUSIONS

In the present work we formulated the problem of non-Darcy natural convection in a metal foam heated from below and validated the model by comparing with published results. In part 2, we apply the model to study the flow and heat transfer characteristics of metallic foam samples .

6. REFERENCES

Amiri, A and K. Vafai, 1994, "Analysis of Dispersion Effects and Non-Thermal Equilibrium, Non-Darcian, Variable porosity Incompressible Flow Through Porous Media", *Int. J. Heat Mass Transfer*, vol. 37, No. 6, pp. 939-954

Amiri, A, Vafai, K. and T.M. Kuzay, 1995, Effects of Boundary Conditions On Non-Darcian Heat Transfer Through Porous Media and Experimantal Comparisons", *Numerical Heat Transfer*, Part A, vol. 27, pp. 651-664

Bear, J., *Dynamics of Fluids in Porous Media*, Dover, New York (1972)

Beckermann, C, Ramadhyani, S., and R. Viskanta, 1987, "Natural Convection Flow and Heat Transfer Between a Fluid Layer and Porous Layer Inside a Rectangular Enclosure", ASME JOURNAL OF HEAT TRANSFER, Vol. 109, pp. 363-370.

Beji, H., Nonlinear effects and influence of thermal dispersion on natural-convection heat-transfer in porous enclosures, Journal de Physique III, 3: (2) 267-284 FEB 1993

Calmidi, V.V., Transport Phenomena in High Porosity Fibrous Metal Foams, Ph.D. Thesis, University of Colorado at Boulder, 1998.

Calmidi, V.V. and R.L. Mahajan, 2000, "Forced Convection in High Porosity Metal Foams", To appear in the ASME J. Heat Transfer.

Calmidi, V.V. and R.L. Mahajan, 1999, "The Effective Thermal Conductivity of High Porosity Fibrous Metal Foams", ASME JOURNAL OF HEAT TRANSFER, Vol. 121, pp. 466-471.

Givler, R.C. and Altobelli, S.A., 1994, "A Determination of the Effective Viscosity for the Brinkman-Forchheimer Flow Model", *J. Fluid Mech*., Vol. 258, pp. 355-370

Gobin, D., Goyeau, B., and J.-P. Songbe, "Double Diffusive Natural Convection in a Composite Fluid-Porous Layer", ASME JOURNAL OF HEAT TRANSFER, Vol. 120, pp. 234-242.

Hunt M.L and C.L. Tien , 1988, Effects Of Thermal Dispersion On Forced-Convection In Fibrous Media, Int. J. Heat Mass Tran 31: (2) 301-309.

Incropera, F.P. 1997, *Introduction to Heat Transfer*, John Wiley & Sons, New York .

Jiang, P.-X., Ren, Z.-P. and B.-X. Wang, "Numerical Simulation of Forced Convection Heat Transfer in Porous Plate Channels Using Thermal Equilibrium and Nonthermal Equilibrium Models", *Numerical Heat Transfer* – Part A, vol. 35, pp.99-113 (1999)

Neale, G. and W. Nader, 1974, "Practical Significance of Brinkman's Extension of Darcy's Law", Can. J. Chem. Engg., 52, pp. 475-478

Nield, D.A. and Kuznetsov, A.V., "Local Thermal Nonequilibrium Effects in Forced Convection in a Porous Medium Channel", *Int. J. Heat Mass Transfer*, 42, pp. 3245-3252 (1999)

Hsiao, S.W., 1998, "Natural convection in an inclined porous cavity with variable porosity and thermal dispersion effects", *Int. J. Numerical Methods For Heat & Fluid Flow*, 8: (1), 97.

Koch, D.L. and J.F. Brady, 1986, "The effective diffusivity of porous media", *AIChE J*., vol. 32, p. 575

Lloyd, J.R. and W.R. Moran, Natural Convection Adjacent yo Horizontal Surfaces of Various Planforms, ASME Paper 74-WA/HT-66, 1974

Patankar, S.V., 1980, *Numerical Heat Transfer and Fluid Flow*, Hemisphere, Washington, D.C.

Sathe, S.B, Peck, R.E and Tong, T.W, 1990, "A Numerical-Analysis of Heat-Transfer And Combustion In Porous Radiant Burners", *Int. J. Heat Mass Transfer*, 33: (6) 1331-1338

Sathe, S.B., W.Q. Lin, and T.W. Tong, 1988, "Natural Convection in Enclosures Containing an Insulation with a Permeable Fluid-Porous Interface", *Int. J. Heat Fluid Flow*, 9, No. 4, pp. 389-395

Vafai, K. and C.L. Tien, 1981, "Boundary and Inertia Effects on Flow and Heat Transfer in Porous Media", *Int. J. Heat Mass Transfer*, 24, pp. 195-203.

Zhukauskas, A., 1972, "Heat transfer from tubes in cross flow", in *Adv. Heat Transfer*, vol. 8, Academic Press, New York.